Available online at www.sciencedirect.com
SCIENCE DIRECT
Journal of Molecular Structure 743 (2005) 103–115
Journal of MOLECULAR STRUCTURE
www.elsevier.com/locate/molstruc

Structural influence on the intermolecular/intramolecular hydrogen bonding in solid state of substituted leflunomides: evidence by X-ray crystal structure

T.K. Venkatachalam[a], Y. Zheng[a], S. Ghosh[b], F.M. Uckun[c,*]

[a]*Department of Chemistry, Parker Hughes Institute, 2685 Patton Road, Roseville, MN 55113, USA*
[b]*Department of Structural Biology, Parker Hughes Institute, 2685 Patton Road, Roseville, MN 55113, USA*
[c]*Department of Virology, Parker Hughes Institute, 2685 Patton Road, Roseville, MN 55113, USA*

Received 15 November 2004; revised 1 February 2005; accepted 14 February 2005

Abstract

We report the results of an X-ray crystal structure study of nine substituted leflunomide metabolite analogs (LFM). Comparison of the hydrogen bonding characteristics exhibited by these structurally distinct LFM analogs was especially informative about the inter- and intra-molecular hydrogen bonding patterns that exist in the crystal structure of individual compounds. All compounds had the strong intramolecular hydrogen bonds. In addition, with the exception of the 2,5-difluorophenyl substituted LFM analog, all other compounds formed inter- or intra-molecular hydrogen bonds with the halogen atom and the NH group. However, we found that the presence of a fluorine atom at the 2-position on the phenyl ring of the 2,5-difluoro and 2-fluoro derivatives resulted in only one intramolecular hydrogen bond in the structural framework. Conversely, the 3,5-difluoro substituted LFM analog had an intramolecular hydrogen bond common to the other halide substituted derivatives. The anomaly exhibited by the 2,5-difluoro and the 2-fluoro substituted compounds may be owing to the smaller size of fluorine atom in comparison with the chlorine and bromine atoms in the structures of the other analogs. The presence of a fluorine at the 2-position of the phenyl ring may disrupt the intermolecular hydrogen bonding that was observed for the other derivatives due to differences in the crystal packing for these molecules.

Keywords: Leflunomides; Crystal structures; Fluorine atom; Hydrogen bonding

1. Introduction

Apoptosis is a common mode of eukaryotic cell death that is triggered by an inducible cascade of biochemical events leading to the activation of endonucleases that cleave the nuclear DNA into oligonucleosome length fragments [1–4]. Several biochemical events contribute to apoptotic cell death. An improved understanding of the molecular basis of apoptosis and the pro-apoptotic versus anti-apoptotic regulatory signals may provide further insight into the pathogenesis of human lymphoid malignancies. Selective inhibitors of the anti-apoptotic tyrosine kinase, BTK hold promise as a new generation of anti-leukemic agents with apoptosis promoting and chemosensitizing properties. The epidermal growth factor receptor (EGFR) is a membrane-associated tyrosine kinase that serves as an endogenous negative regulator of apoptosis in breast cancer cells [5]. Consequently, the development of new potent anti-breast cancer agents has emerged as an important focal point for translational research in the treatment of breast cancer [6]. Recently, compound A77 1726, which is the primary metabolite of the isoxazole leflunomide [*N*-(4-trifluoromethylphenyl)-5-methylisoxazol-4-carboxamide), was shown to possess anti-inflammatory activity with pleiotropic effects [7–10]. Mattar et al. [11] also provided experimental evidence that the above compound inhibited EGFR kinase in micromolar concentrations.

In a systematic search for potent anti-cancer agents, we have identified several structurally distinct LFM analogs as potent inhibitors of tyrosine kinases. In the previous studies, we have examined the X-ray crystal structures of a few LFM analogs [12–16]. In this paper we report a detailed study on

* Corresponding author. Tel.: +1 612 697 9228; fax: +1 612 697 1042.
E-mail address: fatih_uckun@ih.org (F.M. Uckun).

0022-2860/$ - see front matter © 2005 Elsevier B.V. All rights reserved.
doi:10.1016/j.molstruc.2005.02.024

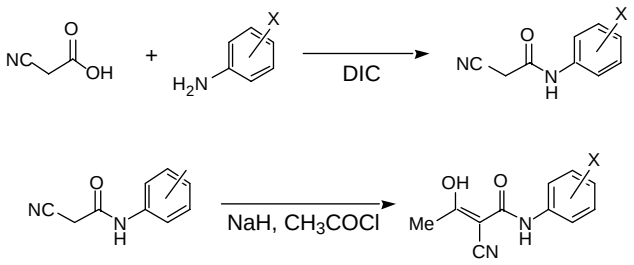

Scheme 1. General synthetic scheme for leflunomide derivatives.

the X-ray crystal structures of several of these LFM analogs and the influence of their structural differences on the anisotropy in intermolecular hydrogen bonding characteristics.

2. Experimental

All chemicals were purchased from Aldrich (Milwaukee, WI) and were used without further purification. Unless otherwise noted, each reaction vessel was secured with a rubber septum, and the reaction was performed under a nitrogen atmosphere. The leflunomide derivatives were prepared using previously published data [13]. The prepared compounds were purified using column chromatography on silica gel, followed by recrystallization. Samples were identified by NMR, IR and UV spectroscopy, mass spectrometry, and analytical HPLC. The ^{1}H and ^{13}C NMR spectra were obtained on a Varian Mercury 300 instrument at ambient temperature in DMSO-d_6. FT-IR spectra were recorded on a Nicolet Protégé 460 spectrometer between 600 and 4000 cm^{-1} as KBr pellets. UV spectra were recorded from a Beckmann DU 7400 UV/Vis spectrometer using a cell path length of 1 cm in methanol. Mass spectra were performed on a Hewlett Packard MALDI-TOF spectrometer (Model G2025A LD-TOF) using dithranol as the supporting matrix. Melting points were determined using a Melt John's apparatus and are uncorrected. HPLC data was collected using a Hewlett Packard 1100 series instrument consisting of an automatic sampler, an electronic degasser, a thermostatic control unit, and a diode array detector in conjunction with a Chemstation software assembly. The column was an analytical RP-18 Lichrospher column (4.6×250 mm^2, 5 μm particle size) and eluent was H_2O (0.1% ACOH):acetonitrile (35:65). The flow rate was maintained at 1.0 ml/min and the detection wavelength was set at 275 nm. The column was maintained at room temperature throughout the analysis.

A detailed procedure for the synthesis of **8** is provided below, and should be considered representative for the synthesis of the lefunomide derivatives presented in this paper.

Synthesis of (2*Z*)-*N*-(2,4-dibromophenyl)-2-cyano-3-hydroxybut-2-enamide (**8**). In a 250 ml RB flask, under a nitrogen atmosphere, cyanoacetic acid (3.4 g, 40 mmol) and 2,4-dibromoaniline (11.0 g, 44 mmol) were fully dissolved in anhydrous tetrahydrofuran (80 ml). To this

Table 1
Structures of LEF compounds

Compound	Structure	Compound	Structure
1	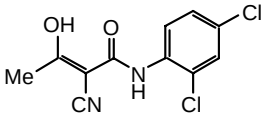	**6**	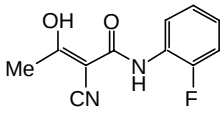
2	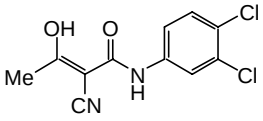	**7**	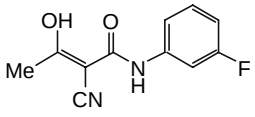
3	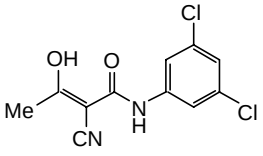	**8**	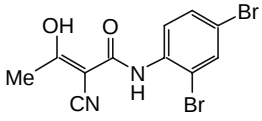
4	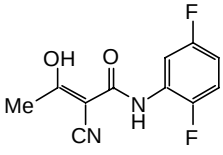	**9**	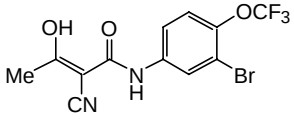
5	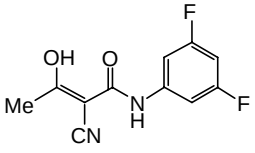	**10**	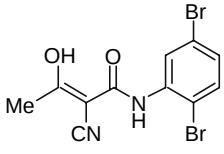

Table 2
Selective crystal data for compounds (Å, deg)

Compound	Space group	*a*	*b*	*c*	*α*	*β*	*γ*
1	*P*-1	5.5089	9.9183	11.8075	68.40	82.59	87.72
2	*P*-1	4.4845	9.5145	13.5388	91.22	95.40	94.00
3	*P*-1	4.4493	9.5719	14.378	77.10	83.75	86.07
4	*P*2(1)/*n*	8.598	5.595	21.407	90.0	92.31	90.0
5	*P*1	4.6397	9.2124	13.0502	75.69	81.71	85.54
6	*P*1	5.2782	10.2335	11.5754	69.79	78.59	75.84
7	$P2_1/c$	4.7724	24.1536	9.1565	90.0	95.94	90.0
8	*C*2/*c*	15.289	12.584	13.714	90.0	108.59	90.0
9	*P*-1	5.2834	10.8265	13.1634	69.01	81.09	83

solution was added 1,3-diisopropylcarbodiimide (6.3 ml, 40 mmol), and the mixture was allowed to stir overnight at room temperature, during which a precipitate was formed. The precipitated urea was removed by filtration and solution partitioned between ethyl acetate and 0.5 N HCl [1:1]. The organic layer was separated from the aqueous layer, washed with brine, and dried over anhydrous sodium sulfate. After filtration and removal of the solvent under vacuum the residue was then crystallized from ethyl alcohol to obtain 12.1 g of *N*-(2,4-dibromophenyl)-2-cyanoacetamide.

In the subsequent step, *N*-(2,4-dibromophenyl)-2-cyanoacetamide (11.1 g, 35 mmol) was dissolved in anhydrous tetrahydrofuran (250 ml) under a nitrogen atmosphere and sodium hydride (3.1 g, 77 mmol) was added carefully to the solution. The mixture was allowed to stir at room temperature for 1 h. After this period, acetyl chloride (3.0 ml, 42 mmol) was slowly added to the reaction mixture. The solution was allowed to stir at room temperature for 1 h, then quenched by adding acetic acid (5 ml). The mixture was poured into ice water (500 ml) containing hydrochloric acid (12.5 ml) to precipitate the crude product. The precipitated product was collected by filtration, washed with water, and dried under vacuum. The product was recrystallized from ethanol to furnish the analytically pure compound (9.8 g, 78% yield).

Crystals of the leflunomide derivatives were grown by dissolving a compound in an organic solvent, which was then allowed to evaporate slowly. The crystals were then mounted carefully using an epoxy glue on a Bruker SMART CCD area detector diffractometer. The following programs were utilized for cell refinement, data reduction, structure solving, and refinement of the structure: SAINT (Bruker 1998a), SHELXTL (Bruker, 1998b) and SHELXS97 [17,18]. The program used to refine the structure was SHELXL [19]. Molecular graphics and publication materials were prepared using SHELXTL.

3. Results and discussion

The target LFM analogs were prepared in a two-step procedure following Scheme 1. In brief, cyanoacetic acid

Table 3
Selected bond and hydrogen bond lengths (Å)

Compound	D–H···A	D–H	H···A	D···A	D–H···A
1	O(9)–H(9)···O(7)	0.81(3)	1.78(3)	2.5329(17)	153(3)
	O(9)–H(9)···O(7)#1	0.81(3)	2.56(3)	3.0477(18)	120(2)
	N(1)–H(1)···Cl(6)	0.80(2)	2.50(2)	2.9434(13)	116.8(19)
2	N(1)–H(1)···N(11)#1	0.87(2)	2.36(2)	3.204(2)	162.0(19)
	O(9)–H(9)···O(7)	0.92(3)	1.70(3)	2.5181(18)	147(2)
	O(9)–H(9)···O(7)#2	0.92(3)	2.46(2)	2.9514(19)	113.7(18)
3	O(9)–H(9)···O(7)	0.96(3)	1.62(3)	2.512(3)	153(3)
	N(1)–H(1)···N(11)#1	0.86	2.34	3.164(3)	161.3
4	O(9)–H(9)···O(7)	0.88(5)	1.70(5)	2.500(5)	150(5)
5	O(9)–H(9)···O(7)	0.82	1.74	2.4802(19)	148.5
	N(1)–H(1)···N(11)#1	0.83(2)	2.33(2)	3.128(2)	161.9(18)
6	O(9)–H(9)···O(7)	0.82	1.81	2.540(2)	147
7	O(9)–H(9)···O(7)	0.98(3)	1.56(3)	2.483(2)	156(2)
	N1–H1···N(11)#1	0.87(2)	2.30(2)	3.134(3)	163(2)
8	O(9)–H(9)···O(7)	0.84(4)	1.70(5)	2.509(3)	161(5)
	N(1)–H(1)···Br(2)	0.77(3)	2.54(3)	3.056(3)	126(3)
9	O(9)–H(9)···O(7)	0.89(6)	1.70(6)	2.508(4)	150(5)
	O(9)–H(9)···O(7)#1	0.89(6)	2.52(5)	3.027(4)	117(4)
	N(1)–H(1)···N(11)#2	0.82(3)	2.44(4)	3.218(5)	161(3)

Compound **1**, symmetry code: $-x-1$, $-y$, $-z+1$. Compound **2**, symmetry code #1: $-x+3$, $-y+1$, $-z+1$; symmetry code #2: $-x+1$, $-y$, $-z+1$. Compound **3**, symmetry code #1: $-x+2$, $-y$, $-z+1$. Compound **5**, symmetry code: $-x+2$, $-y$, $-z+2$. Compound **7**, symmetry code: $-1-x$, $1-y$, $1-z$. Compound **9**, symmetry code#1: $-x+1$, $-y$, $-z$; symmetry code #2: $-x+2$, $-y+1$, $-z$.

was condensed with substituted aniline in presence of diisopropylcabodiimide to furnish the substituted amide. This amide was further treated with sodium hydride and acylated using acylchloride to obtain the desired leflunomide.

The structures of the compounds analyzed in this study are provided in Table 1. Halide substituents on the phenyl group were focused on as these compounds were found to be biologically active [13]. We first compared the crystal structures of similarly substituted LFM analogs for any changes in the crystal structure characteristics. Accordingly, compounds **1**–**3** are the compounds possessing 2,4-dichloro, 3,4-dichloro and 3,5-dichloro substituents, respectively, on the phenyl ring. All three were triclinic with a *P*-1 space group. Selected crystal data determined for these compounds is provided in Table 2. In addition, Table 3 provides the hydrogen bonds and their length, and Tables 4 and 5 show selected bond lengths and angles for all the derivatives. Figs. 1–3 show the X-ray crystal structures of these three compounds along with their respective crystal packing diagram.

The crystal structure of **1** revealed two intramolecular hydrogen bonds, one between the C═O and O–H group and one for the N–H near the phenyl ring and the chloride at the 2-position of the phenyl ring, [O(9)–H(9)···O(7) = 2.5329(17) and N(1)–H(1)···Cl(6) = 2.9434(13)] (Table 3). The hydrogen bonds can be expressed in graph set motif form as $S_1^1(6)$ and $S_1^1(5)$

Table 4
Selected bond lengths

Compound	Atom designation	Bond length (Å)
1	Cl(4)–C(4)	1.7425(17)
	Cl(6)–C(6)	1.7360(15)
	O(7)–C(7)	1.2376(17)
	O(9)–C(9)	1.313(2)
	N(11)–C(11)	1.138(2)
2	Cl(3)–C(3)	1.7294(17)
	Cl(4)–C(4)	1.7342(17)
	O(7)–C(7)	1.249(2)
	O(9)–C(9)	1.319(2)
	N(11)–C(11)	1.141(2)
3	Cl(3)–C(3)	1.744(3)
	Cl(5)–C(5)	1.743(3)
	O(7)–C(7)	1.254(3)
	O(9)–C(9)	1.325(3)
	N(11)–C(11)	1.141(3)
4	F(3)–C(3)	1.355(5)
	F(6)–C(6)	1.345(5)
	O(7)–C(7)	1.230(5)
	O(9)–C(9)	1.304(5)
	N(11)–C(11)	1.132(6)
5	F(3)–C(3)	1.352(2)
	F(5)–C(5)	1.362(2)
	O(7)–C(7)	1.249(2)
	O(9)–C(9)	1.310(2)
	N(11)–C(11)	1.138(2)
6	F(2)–C(2)	1.359(30
	O(9)–C(9)	1.319(3)
	O(7)–C(7)	1.246(3)
7	F(5)–C(5)	1.355(3)
	O(7)–C(7)	1.249(2)
	O(9)–C(9)	1.315(2)
8	Br(2)–C(2)	1.900(3)
	Br(4)–C(4)	1.907(3)
	O(7)–C(7)	1.245(3)
	O(9)–C(9)	1.316(4)
	N(11)–C(11)	1.130(4)
9	Br(1)–C(5)	1.884(4)
	F(1)–C(12)	1.288(7)
	F(2)–C(12)	1.305(6)
	F(3)–C(12)	1.286(7)
	O(7)–C(7)	1.241(5)
	O(9)–C(9)	1.320(5)
	N(11)–C(11)	1.134(5)

Table 5
Selected bond angles

Compound	Bond designation	Angles (deg)
1	C(7)–N(1)–C(1)	128.81(13)
	O(7)–C(7)–N(1)	123.40(14)
	C(11)–C(8)–C(7)	119.16(13)
	O(9)–C(9)–C(8)	121.66(15)
	N(11)–C(11)–C(8)	175.96(18)
2	C(7)–N(1)–C(1)	128.17(14)
	O(7)–C(7)–N(1)	122.53(15)
	C(11)–C(8)–C(7)	121.06(14)
	O(9)–C(9)–C(8)	121.87(15)
	N(11)–C(11)–C(8)	179.40(2)
3	C(7)–N(1)–C(1)	128.4(2)
	O(7)–C(7)–N(1)	122.1(2)
	C(11)–C(8)–C(7)	121.2(2)
	O(9)–C(9)–C(8)	121.5(2)
	N(11)–C(11)–C(8)	179.6(3)
4	C(7)–N(1)–C(1)	128.3(4)
	O(7)–C(7)–N(1)	121.7(4)
	C(11)–C(8)–C(7)	120.7(4)
	O(9)–C(9)–C(8)	121.5(4)
	N(11)–C(11)–C(8)	178.4(5)
5	C(7)–N(1)–C(1)	127.69(15)
	O(7)–C(7)–N(1)	122.09(17)
	C(11)–C(8)–C(7)	121.39(17)
	O(9)–C(9)–C(8)	121.55(17)
	N(11)–C(11)–C(8)	179.4(2)
6	C(7)–N(1)–C(1)	128.8
	O(7)–C(7)–N(1)	121.8
	C(11)–C(8)–C(7)	119.8
	O(9)–C(9)–C(8)	122.2(2)
	N(11)–C(11)–C(8)	178.0(3)
7	C(7)–N(1)–C(1)	127.5(17)
	O(7)–C(7)–N(1)	122.3(19)
	C(11)–C(8)–C(7)	121.7(17)
	O(9)–C(9)–C(8)	121.6(19)
	N(11)–C(11)–C(8)	179.6(2)
8	C(7)–N(1)–C(1)	130.1(3)
	O(7)–C(7)–N(1)	122.40(3)
	C(11)–C(8)–C(7)	119.0(3)
	O(9)–C(9)–C(8)	121.2(3)
	N(11)–C(11)–C(8)	176.1(4)
9	C(7)–N(1)–C(1)	128.8(4)
	O(7)–C(7)–N(1)	122.7(4)
	C(11)–C(8)–C(7)	120.2(3)
	O(9)–C(9)–C(8)	121.0(4)
	N(11)–C(11)–C(8)	177.9(4)

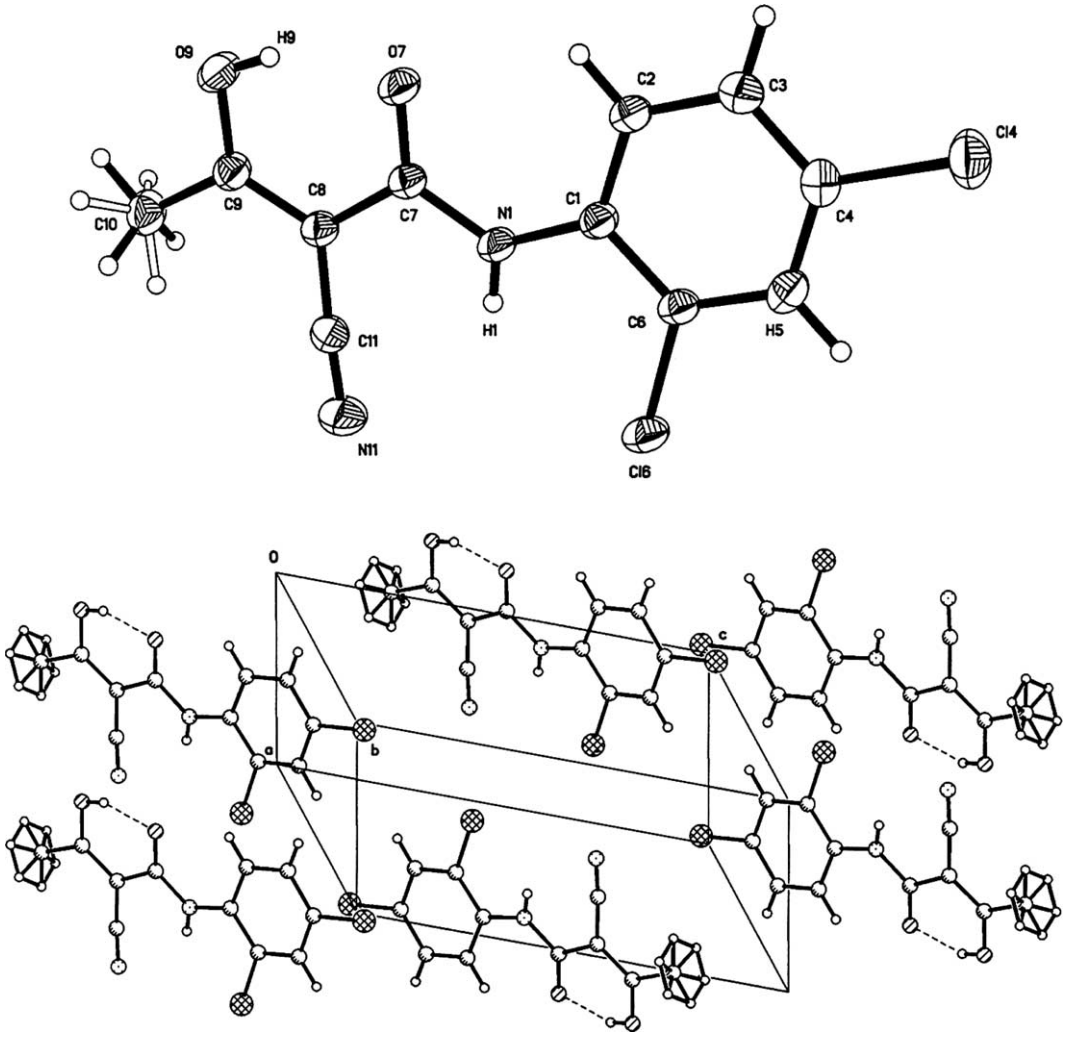

Fig. 1. X-ray crystal structure of **1** and its crystal packing diagram.

that imparts a more rigid conformation to the molecule. These intramolecular hydrogen bonds are present forming a six-member ring and a five-member ring. The molecule is represented below in the graph set motif form in Scheme 2.

Formation of an intramolecular hydrogen bond between C═O and O–H was expected due to the higher electronegative character of the oxygen atom. Furthermore, the formation of intramolecular hydrogen bond between the chlorine and the N–H would eliminate the availability of the N–H hydrogen for additional hydrogen bonding. The formation of an N–H–Cl hydrogen bond would allow the molecule to be highly planar and it would also provide a balance between two rings, one at the top of the plane and the other at the bottom. This hydrogen bond stabilizes the molecule to a rigid structure due to the presence of five and six membered rings. In other words, the free rotation around C–NH bond attached to the phenyl ring appeared to be curtailed due to this hydrogen bond. The compound exhibited an intermolecular hydrogen bonding between O–H and C═O in the crystal structure (Table 3). No intermolecular hydrogen bonding was observed between the second chloride at the 4-position with another molecule.

Compound **2**, a 3,4-dichlorophenyl substituted LFM analog displayed an intramolecular hydrogen bond between the C═O and O–H group similar to that observed for **1**. There was no intramolecular hydrogen bond with chlorine atom likely due to the positional change of chlorine atoms in the structure of the molecule. Of interest, this compound did show an intermolecular hydrogen bond between CN and N–H as shown in the following graph set motif form $R_2^2(12)$ with a 12 member ring formation (Scheme 3).

This compound also formed a second intermolecular hydrogen bond with C═O and O–H as seen in **1**.

Compound **3**, which has a 3,5-dichloro substituent on the phenyl ring, formed an intramolecular hydrogen bond between C═O and O–H very similar to that observed for compounds **1** and **2**. Once again, in the absence of a chlorine atom at the 2-position on the phenyl ring, the N–H formed a hydrogen bond with the CN intermolecularly. In addition a third hydrogen bond with intermolecular hydrogen bonding was observed with C═O and O–H as expected

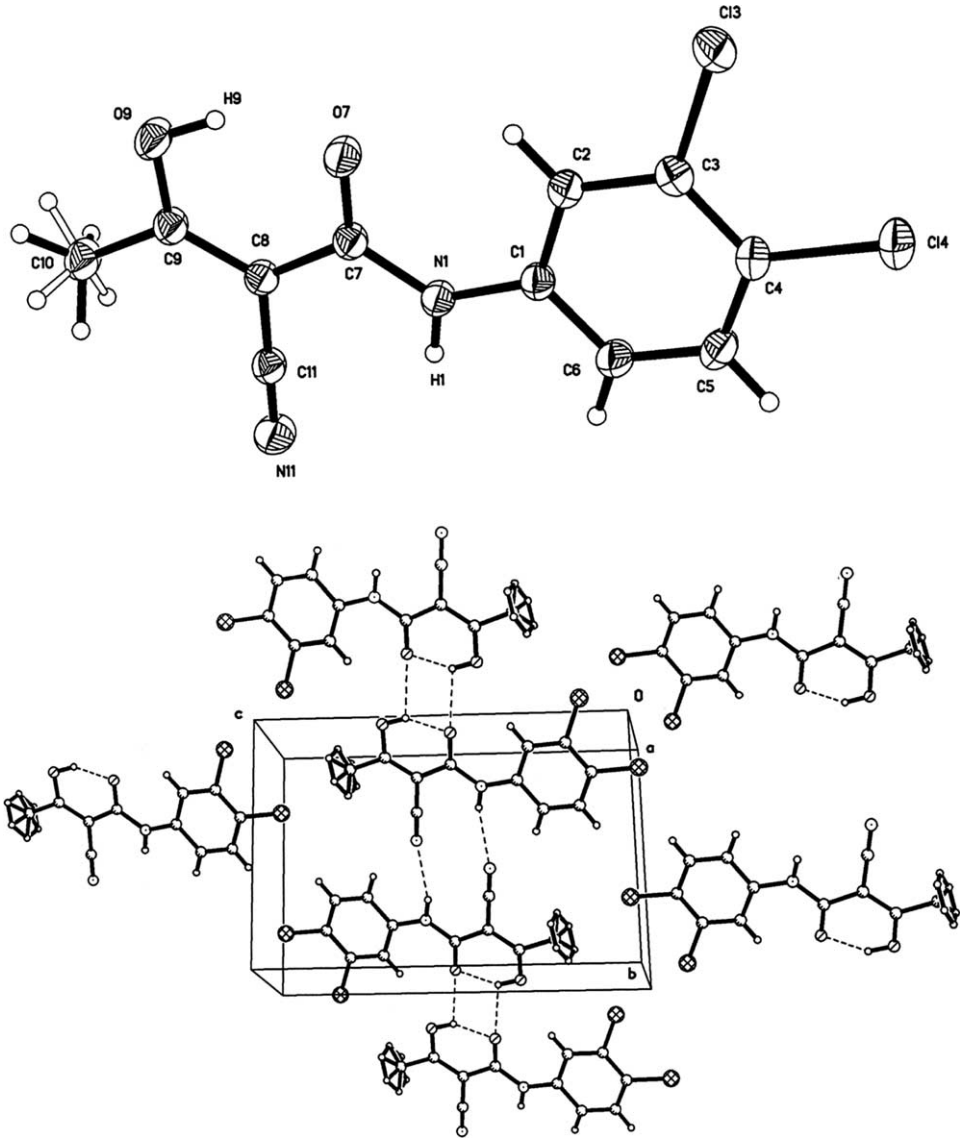

Fig. 2. X-ray crystal structure of **2** and its crystal packing diagram.

(Fig. 3). The graph set motif form of this compound is represented in Scheme 4.

Compounds **1**–**3** each formed intermolecular hydrogen bonds between the N–H and CN groups. In addition, the O–H and C═O of individual molecules also formed intermolecular hydrogen bonding in their solid state. However, only **1** had an intramolecular hydrogen bond with the chlorine atom likely due to its location at the 2-position on the phenyl ring. This aspect will be clear when we consider other substituents at the 2-position of the phenyl ring in the following discussion.

We extended our work by examining the crystal structure of structurally similar compounds **4** and **5** (Figs. 4 and 5). In both compounds there is a fluorine substitution on the phenyl ring. Compound **4** formed a monoclinic crystal and had only one intramolecular hydrogen bond, which was between the C═O and the O–H groups. Notably, there were no other hydrogen bonds present in the crystal structure of the compound. This is of note since one would have expected an intramolecular hydrogen bond between a 2-position fluoride and the N–H group similar to that observed with the 2,4-dichloro substituted compound (**1**). The absence of this intramolecular hydrogen bond for this compound could probably be best explained by considering the size of the fluoride in relation to that of chloride, since both of them are highly electronegative in character. Further comparison of the torsion angle data for these compounds show that a twisting structure is also not the cause for this behavior. The torsion angle only varied within −2.0–7.9° for all the compounds (Table 6). Recently, Yogavel et al. [20] examined the crystal structure of 2-cyano-3-dimethylamino-*N*-(4-methylphenyl)acrylamide and 2-cyano-3-dimethylamino-*N*-(2-methoxyphenyl)acrylamide and found that the hydrogen bond formation occurs between

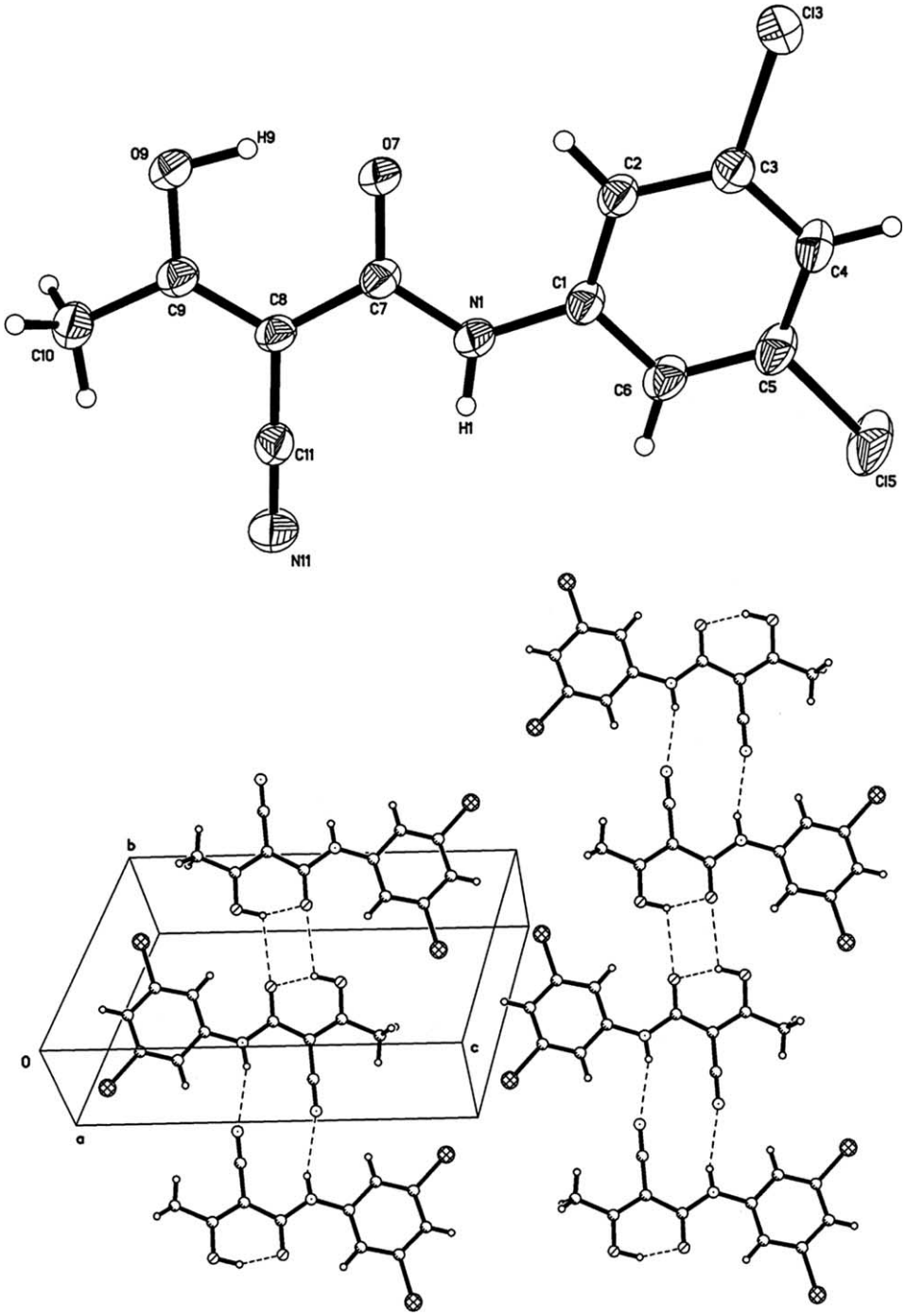

Fig. 3. X-ray crystal structure of **3** and its crystal packing diagram.

the methoxy group and N–H. This was further explained due to the difference in torsion angles associated with certain bonds of these two compounds [−3.7(3) and −20.2(2)°]. In our example, the torsion angles for individual compounds for C(7)–N(1)–C(1)–C(2) bond were **1**, −7.7(3); **2**, −6.1(3); **3**, 7.9(4); **4**, −2.5(7); **5**, 4.2; **8**, 2.7(5); **9**, −2.0(7). There was also no evidence of an intermolecular hydrogen bond between N–H and CN of **4**, again in contrast to what was observed for the chloro

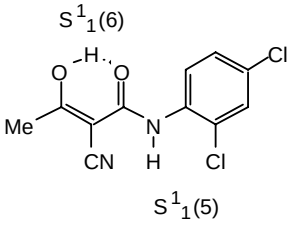

Scheme 2. Graph set motif of **1**.

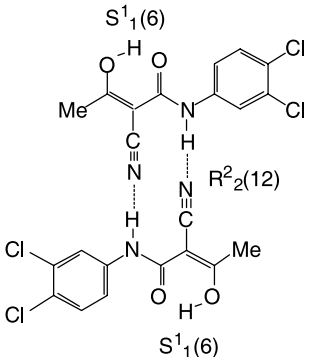

Scheme 3. Graph set motif of **2**.

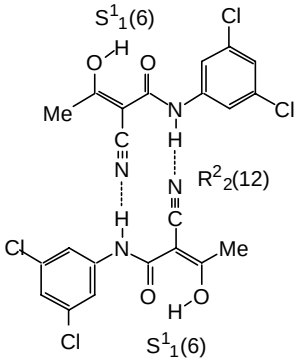

Scheme 4. Graph set motif of **3**.

compound. Additionally, we found that there was no intermolecular C═O and O–H hydrogen bond formation either. Scheme 5 shows the graph set motif representation of the molecule.

Having established that a 2,5-difluoro substituted LFM analog does not form inter- and intramolecular hydrogen bonds, we next examined the crystal structure of 3,5-difluoro substituted compound (**5**) (Fig. 5) to compare its characteristics with those of the corresponding 3,5-dichloro compound. Examining the crystal structure we found one intramolecular hydrogen bond between the C═O and O–H group. In contrast to compound **4**, compound **5** had an intermolecular hydrogen bond between the CN and N–H groups of the molecule as represented below in the graphic set motif form (Scheme 6). However, we did not observe additional intermolecular hydrogen bonding involving C═O and O–H, which was present in the chloro substituted compounds as discussed before.

It appears that the presence of a fluorine atom at the 2-position of the phenyl ring may disrupt the intermolecular hydrogen bonds between the CN and N–H groups, as well as the intermolecular hydrogen bonds between the C═O and O–H groups in the crystal lattice. On the other hand, when the fluoro atom is present in a different position of the phenyl ring the usual inter- and intra-molecular hydrogen bonds typical of these compounds are observed in the crystal structure. Another example of this structural relationship is found in the previously reported 2-fluoro phenyl substituted LFM analog (**6**) which has only a C═O

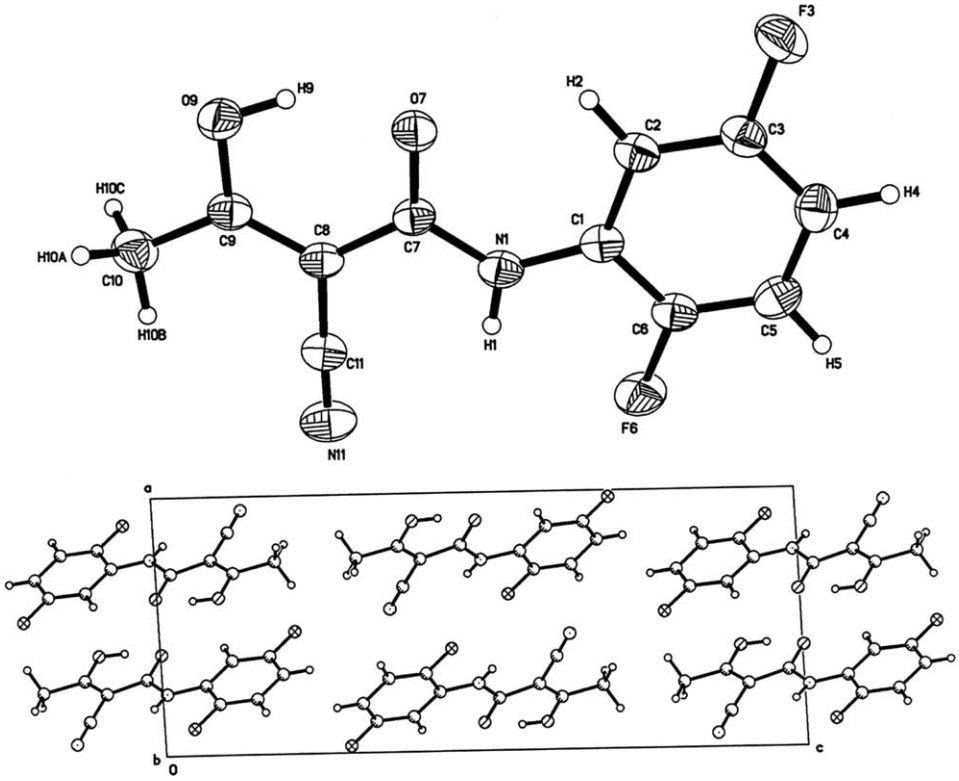

Fig. 4. X-ray crystal structure of **4** and its crystal packing diagram.

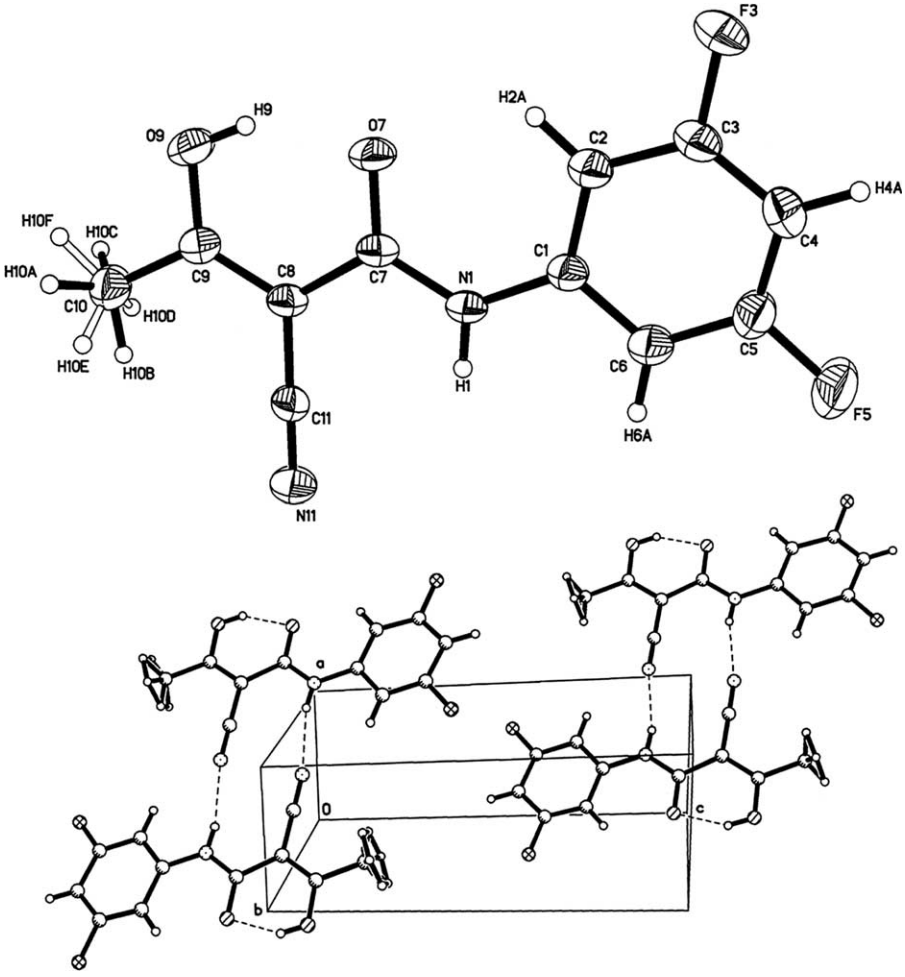

Fig. 5. X-ray crystal structure of **5** and its crystal packing diagram.

and O–H intramolecular hydrogen bond. As with compound **4**, all other hydrogen bonds were absent (Scheme 7) [16]. Hence, the 2-fluoro compounds differed from the 2-chloro substituted analogs.

We also examined the X-ray crystal structure of a 3-fluoro substituted leflunomide analog (**7**) for comparison. This compound had an intramolecular hydrogen bond between C═O and O–H and also an intermolecular hydrogen bond with CN and N–H groups as shown in the graph set motif form (Scheme 8). This provides evidence that the fluorine atom at the 2-position and not merely the presence of a fluorine on the phenyl ring has a remarkable tendency to disrupt these intermolecular hydrogen bonds in the crystal lattice.

To explain the influence of a 2-positioned fluorine on the hydrogen bonding in the crystal lattice we compared the torsion angles of all LFM analogs. Table 6 provides the torsion angles determined for the bonds of interest in the crystal structures of the compounds. From the values it is evident that there was no significant differences in the torsion angles observed in most of the halo-substituted leflunomide derivatives. This result demonstrates that the torsion angle does not influence either the absence or presence of the intramolecular hydrogen bond in these derivatives.

From the previous discussion, we have established that the chloro and fluoro compounds can behave differently in their capacity to form inter- and intra-molecular hydrogen bonds in their solid state. We sought to determine whether the corresponding bromo compound would behave similar to that of the chloro or the fluoro derivative. The 2,4-dibromo substituted leflunomide (**8**) showed two intramolecular hydrogen bonds between C═O and O–H as well as N–H and Br groups (Fig. 6). This trend is similar to that exhibited by the chloro compound and is represented below in the graphic motif form (Scheme 9).

However, the compound did not show any intermolecular hydrogen bonding with CN group and N–H as expected. Both the chloro and bromo compounds indicated identical hydrogen bonding characteristics in their solid state. Also we can rationalize that the size of the bromide is larger and hence it forms the intramolecular hydrogen bond in the crystal lattice. Additionally, it shows the absence of intermolecular hydrogen bond between the CN and N–H

Table 6
Selected torsion angles

Compound	Bond designation	Torsion angle (deg)
1	C(7)–N(1)–C(1)–C(2)	−7.7(3)
	C(7)–N(1)–C(1)–C(6)	173.81(15)
	N(1)–C(1)–C(6)–Cl(6)	0.8(2)
	C(1)–N(1)–C(7)–C(8)	179.06(14)
	N(1)–C(7)–C(8)–C(11)	3.12(2)
2	C(7)–N(1)–C(1)–C(2)	−6.1(3)
	C(7)–N(1)–C(1)–C(6)	174.9(17)
	C(1)–N(1)–C(7)–C(8)	−178.32(15)
	N(1)–C(7)–C(8)–C(11)	0.7(2)
3	C(7)–N(1)–C(1)–C(2)	7.9(4)
	C(7)–N(1)–C(1)–C(6)	−172.6(3)
	C(1)–N(1)–C(7)–C(8)	178.6(3)
	N(1)–C(7)–C(8)–C(11)	−1.6(4)
4	C(7)–N(1)–C(1)–C(2)	-2.5(7)
	C(7)–N(1)–C(1)–C(6)	178.5(4)
	N(1)–C(1)–C(6)–F(6)	0.0(6)
	C(1)–N(1)–C(7)–C(8)	179.7(4)
	N(1)–C(7)–C(8)–C(11)	0.8(6)
5	C(7)–N(1)–C(1)–C(2)	4.2(3)
	C(7)–N(1)–C(1)–C(6)	−176.22(18)
	C(1)–N(1)–C(7)–C(8)	177.64(17)
	N(1)–C(7)–C(8)–C(11)	1.1(3)
8[a]	C(7)–N(1)–C(1)–C(2)	−177.4(3))
	C(7)–N(1)–C(1)–C(6)	2.7(5)
	N(1)–C(1)–C(2)–Br(2)	−1.8(4)
	C(1)–N(1)–C(7)–C(8)	178.9(3)
	N(1)–C(7)–C(8)–C(11)	0.1(4)
9	C(7)–N(1)–C(1)–C(2)	−2.0(7)
	C(7)–N(1)–C(1)–C(6)	178.1(4)
	C(1)–N(1)–C(7)–C(8)	179.7(4)
	N(1)–C(7)–C(8)–C(11)	−0.8(6)

[a] The carbon on the phenyl ring is numbered different in the X-ray crystal structure.

groups for the similar reason that the hydrogen atom is not available. In summary, our results demonstrates that 2-chloro or 2-bromo substituted leflunomide derivatives have the tendency to form intramolecular hydrogen bonds with N–H group, where as the 2-fluoro group disrupts the formation of the intramolecular hydrogen bond.

We completed the study by examining the crystal structure of another bromo-substituted compound (**9**). The reason for choosing this compound was to observe whether introduction of additional group such as OCF_3 on the phenyl ring has any influence on the hydrogen bond formation. The X-ray crystal structure of the compound is shown in Fig. 7. Compound **9** had two hydrogen bonds similar to those exhibited by the other chloro and bromo compounds discussed previously. This compound also formed the intermolecular hydrogen bonding, however, there was no

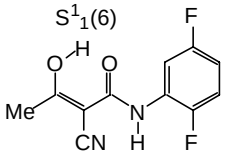

Scheme 5. Graph set motif of **4**.

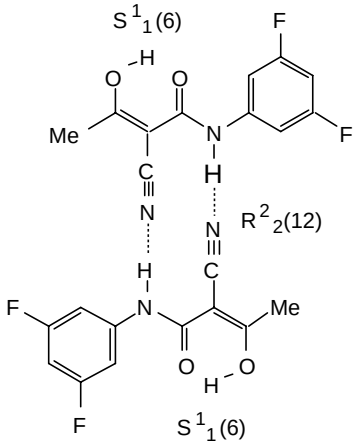

Scheme 6. Graph set motif of **5**.

evidence of hydrogen bonding through the OCF_3 of the molecule.

Overall, our results demonstrates that 2-chloro or 2-bromo substituted leflunomide derivatives have the tendency to form intramolecular hydrogen bonds with N–H group, where as the 2-fluoro group disrupts the formation of the intramolecular hydrogen bond.

In previous discussion, we have demonstrated that chloride and bromide groups will form intramolecular hydrogen bonds with the NH group, while fluoride does not. We propose that this is due to the smaller size of the fluorine in comparison with the other halogens. The observed atomic volume for all the three halogen are as follows: F 17.1 cm^3; Cl 22.7 cm^3; Br 23.5 cm^3 [21]. Comparing the bond lengths of carbon–halogen bonds, it is known that in general carbon–halogen bond increases as we proceed from fluorine

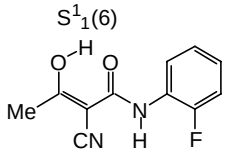

Scheme 7. Graph set motif of **6**.

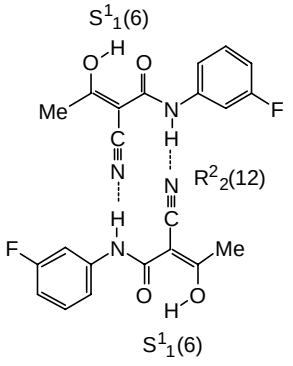

Scheme 8. Graph set motif of **7**.

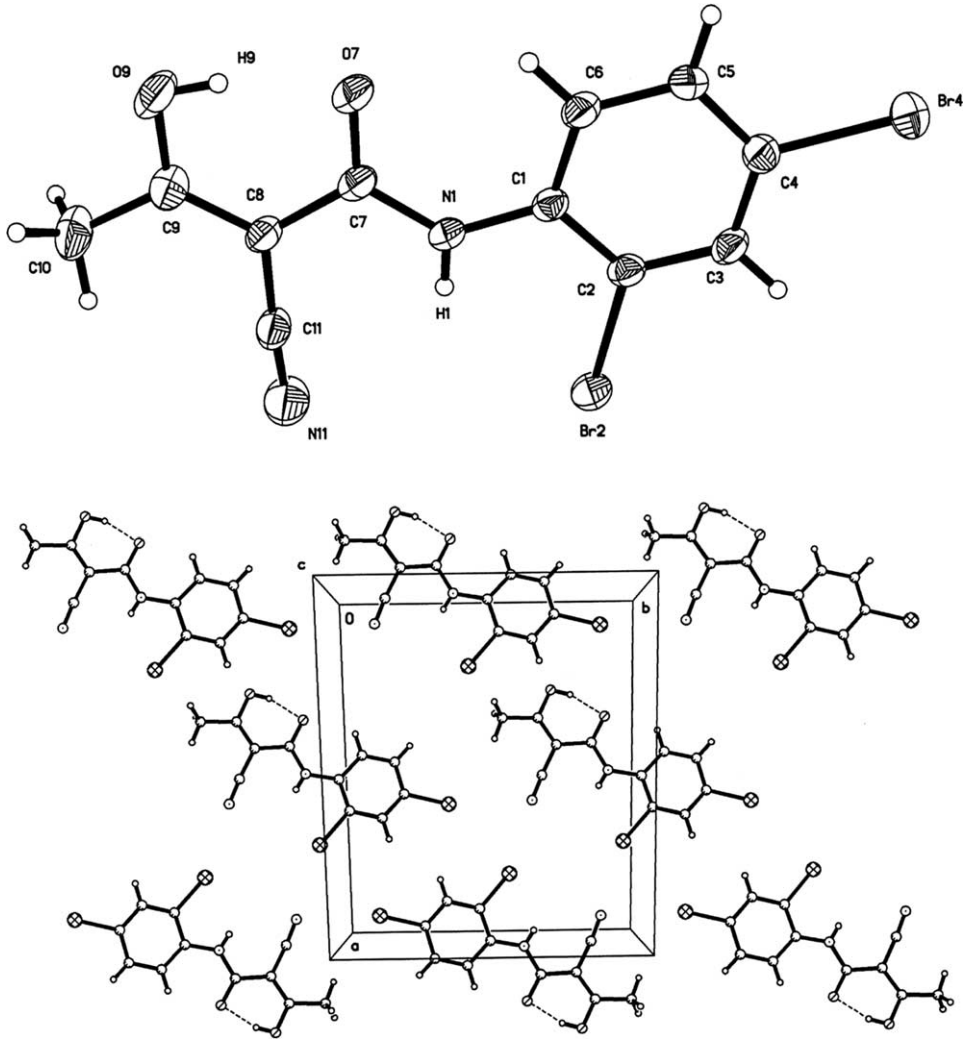

Fig. 6. X-ray crystal structure of **8** and its crystal packing diagram.

to iodine and the values are as follows: C–F 1.39 A, C–Cl: 1.78, C–Br: 1.93, C–I: 2.14. The carbon–halogen bond lengths of lefulonamide analogs are presented in Table 4. The observed values of the bond lengths of carbon–halogen bonds are consistent with the values described above. Based on these bond lengths, we conclude that there is less opportunity for the fluoride to form a hydrogen bond with the NH group due to its relatively shorter bond length. In summary we propose that all the above factors may influence hydrogen bond formation of fluorine with NH, in comparison with other halogens.

3.1. Biological activity of leflunomide analogs

As part of our on-going program in structure-based design of Bruton tyrosine kinase (BTK) inhibitors, we have designed and synthesized several leflunomide metabolite (LFM) analogs, targeting the adenosine triphosphate (ATP) binding site of BTK. The compounds were rationally designed based on the X-ray crystal structure of the BTK kinase domain (Fig. 8). The molecule was docked inside the binding site of BTK. Fig. 8 shows a ball and stick model of the BTK inhibitor LFM-A13 and illustrates the favorable orientation of this molecule in the kinase active site of BTK. The figure was first published by our group and the details of the interaction with various amino acid residues in the BTK site have been discussed previously [13]. The initial lead compound was the 2,5-dibromo compound (LFM-A13, 10) for which we estimated

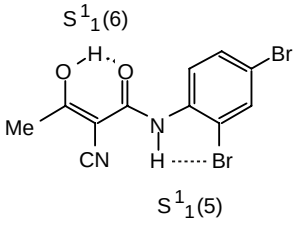

Scheme 9. Graph set motif of **8**.

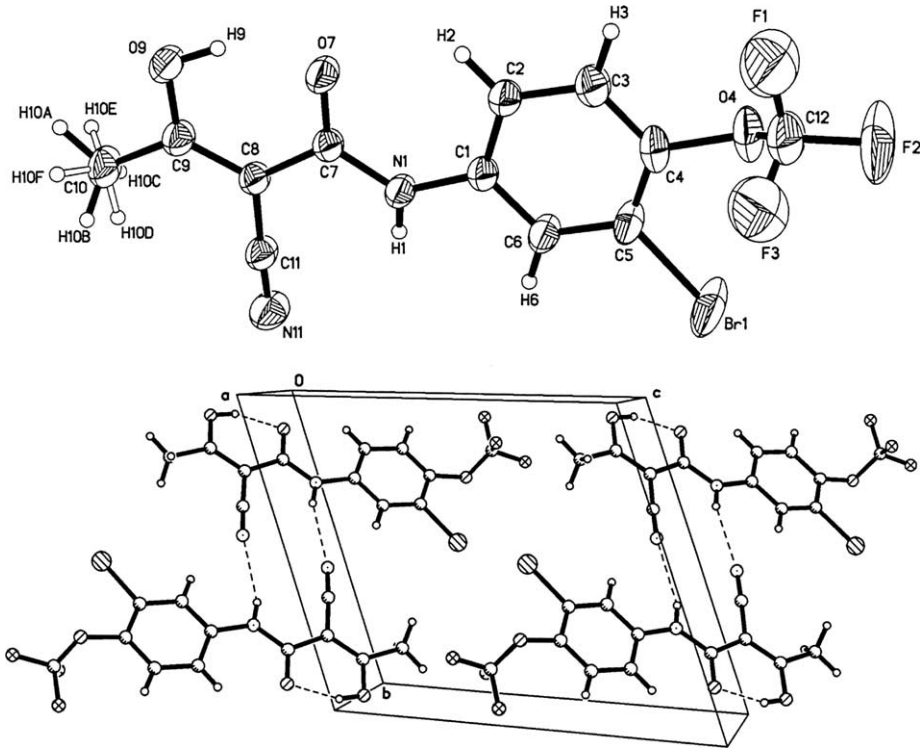

Fig. 7. X-ray crystal structure of **9** and its crystal packing diagram.

a binding constant (K_i) value of 1.4 μM. It inhibited human BTK in vitro with an inhibition (IC_{50}) value of 17.1 ± 0.8 μM and recombinant BTK expressed in a baculovirus expression vector system with an IC_{50} value of 2.5 μM. We have also examined the biological activity of **6** and **7** against EGFR. Compound **6** showed inhibitory activity against EGFR with an $IC_{50} = 74.5$ μM. The overall structure–activity studies revealed that *ortho* substitutions in the phenyl ring would prevent the leflunomide metabolite analog from having a close contact with the hinge region of the EGF receptor kinase domain. Docking studies indicated that *meta* substitutions are likely sandwiched between residues Thr^{766} and Asp^{831}. Finally, the *para* substituted compounds maintain a close contact with the hinge region of the EGFR kinase domain and are stabilized by additional contact area through the *para* substituents and the residues at the inner core of the protein [22].

Most of the leflunomides formed intramolecular hydrogen bonds between the hydroxyl group and the amide carbonyl group. In addition, the crystal packing showed an additional weak intermolecular hydrogen bond between the hydroxyl group and the amide carbonyl-O atom of the centrosymmetrically related molecule. Our study revealed the above compound showed that its molecular conformation is very similar to its corresponding energy-minimized molecular coordinates which were generated and used for docking studies with BTK.

4. Conclusion

In conclusion, we have shown that the structural variation in the leflunomide imparts molecular anisotropy in solid state by preferentially forming inter- and intramolecular hydrogen bonds. We have identified that 2-fluoro substituted compounds have significantly different hydrogen bonding schemes than other leflunomide derivatives with different substitutions on the phenyl group. Additionally, we have shown that there is no significant influence of torsion angles towards this difference in hydrogen bonding

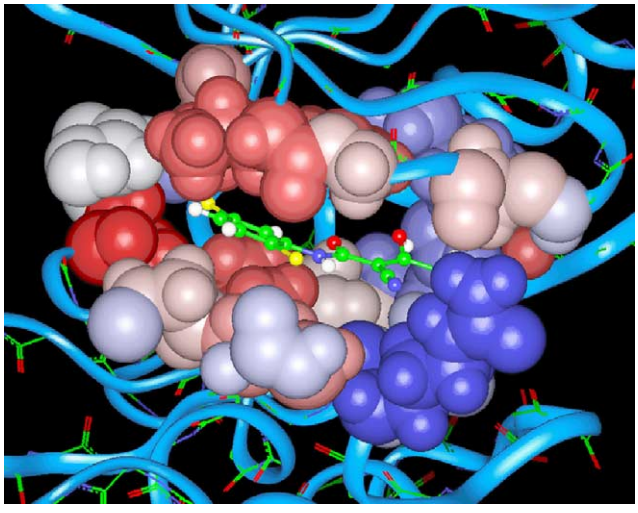

Fig. 8. BTK inhibitor compound **10** docked in the active kinase domain.

characteristics. The difference in hydrogen bonding characteristic shown by fluoro derivatives can be rationalized due to the fluorine's small size as compared to the other halogens. We also propose that the smaller C–F bond lengths may be responsible for its inability to form hydrogen bond with the NH group compared to other halogen substituted compounds. However, the absence of the CN and N–H intermolecular bonding in the case of 2-fluoro substituted leflunomide may be due to the crystal packing characteristic in solid state.

5. Crystallographic data

CCDC 152626, and 252811–252816 contain the supplementary crystallographic data for this paper. These data can be obtained free of charge via www/ccdc/cam/ac/uk/conts/retrieving.html (or from the Cambridge Crystallographic Data Centre, 12, Union Road, Cambridge CB2 1EZ, UK; fax: +44 1223 336033). Deposited data may be accessed by the journal and checked as part of the refereeing process.

References

[1] A.H. Whyllie, J.F. Kerr, A.R. Currie, Int. Rev. Cytol. 68 (1980) 251.
[2] H. Steller, Science 267 (1995) 1445.
[3] A. Fraser, G. Evan, Cell 85 (1996) 781.
[4] S.J. Korsmeyer, Trends Genet. 11 (1995) 101.
[5] F.M. Uckun, R.K. Narla, X. Jun, T. Zeren, T.K. Venkatachalam, K.G. Waddick, A. Rostostev, D.E. Meyers, Clin. Cancer Res. 4 (1998) 901.
[6] J.S. Abrams, T.D. Moore, M. Friedman, Cancer 74 (1994) 1164.
[7] M.J. Parnham, Exp. Opin. Invest. Drugs 4 (1995) 777.
[8] X. Xu, J.W. Williams, E.G. Bremer, A. Finnegan, A.S. Chong, J. Biol. Chem. 270 (1995) 121398.
[9] X. Xu, J.W. Williams, H.G. BertoGong, A. Finnegan, A.S. Chong, Biochem. Pharmacol. 52 (1996) 527.
[10] G. Bertolini, M. Aquino, M. Biffi, G. d'Atri, F. Di Pierro, F. Ferrario, P. Mascagni, F. Somenzi, A. Zaliani, F. Leoni, J. Med. Chem. 40 (1997) 2011.
[11] T. Mattar, K. Kochhar, R. Bartlett, E.G. Bremer, A. Finnegan, FEBS Lett. 334 (1993) 161.
[12] S. Ghosh, Y. Zheng, X. Jun, R. Narla, S. Mahajan, C. Navara, C. Mao, E. Sudbeck, F.M. Uckun, Clin. Caner Res. 4 (1998) 2657.
[13] S. Mahajan, S. Ghosh, E.A. Sudbeck, Y. Zheng, S. Downs, M. Hupke, F.M. Uckun, J. Biol. Chem. 274 (1999) 9587.
[14] S. Ghosh, F.M. Uckun, Acta Crystallogr. C55 (1999) 1364.
[15] S. Ghosh, J.D. Jennissen, Y. Zheng, F.M. Uckun, Acta Crystallogr. C56 (2000) 1254.
[16] S. Ghosh, Y. Zheng, F.M. Uckun, Acta Crystallogr. C55 (1999) 2117.
[17] G.M. Shldrick, Acta Crystallogr. A 46 (1990) 467.
[18] G.M. Sheldrick, SADABS, University of Gottingen, Germany, 1996.
[19] G.M. Sheldrick, SHELXL97, Univeristy of Gottingen, Germany, 1997.
[20] M. Yogavel, P.G. Arvindan, D. Velmurugan, K. Sekar, S. Selvi, P.T. Perumal, S. Shanmuga Sundara Raj, H.K. Fun, Acta Crystallogr. C59 (2003) 394.
[21] E. Prince (Ed.), third ed., International Tables for Crystallography, vol. C, Kluwer Academic Publishers, Dordrecht, The Netherlands, 2004.
[22] S. Ghosh, X.P. Liu, Y. Zheng, F.M. Uckun, Curr. Cancer Drugs Targets 1 (2001) 129–140.